Food Hydrocolloids 129 (2022) 107657

Contents lists available at ScienceDirect

Food Hydrocolloids

journal homepage: www.elsevier.com/locate/foodhyd

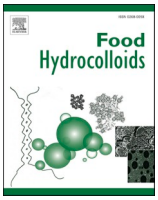

pH-responsive delivery of rebaudioside a sweetener via mucoadhesive whey protein isolate core-shell nanocapsules

Benjamin Pomon, Seyed Mohammad Davachi, Peilong Li, Mohammad Arshadi, Seyedeh S. Madarshahian, Younas Dadmohammadi, Chen Tan, Michelle C. Lee, Zhong Zhang, Ryan D. Woodyer, Rob M. Kriegel, Christopher P. Mercogliano, Alireza Abbaspourrad *

Department of Food Science, College of Agricultural and Life Sciences, Cornell University, Stocking Hall, Ithaca, NY, 14853, USA

ARTICLE INFO

Keywords:
Encapsulation
Interfacial complexation
Steviosides
Ultrasonication

ABSTRACT

Rebaudioside (Reb A) is a natural high-intensity sweetener available for commercial use. Its application has been hampered, however, by its unnatural sweetness profile and a bitter aftertaste at higher concentration thresholds. The goal of this research was to mitigate these shortcomings by increasing the sweetening power, thus lowering the amount needed to achieve the desired sweetness, specifically in acidic liquid media. We achieved the stated goal via the fabrication of a mucoadhesive delivery vehicle that can be retained on the tongue mucosa and allowed for a more targeted and prolonged release of the sweetener near the taste bud. We have chosen hydrolyzed whey protein isolate and pectin as shell materials and crosslinked them via an ultrasonic process. In the pursuit of our goal, we found that WPI-Pectin was the most suitable of all the protein-polysaccharide combinations tested, yielding nanocapsules with average particle sizes of 393 nm and polydispersity index (PDI) of 0.43. These capsules could be resuspended in water with ζ-potential of −20.4 mV. The WPI-pectin system was also shown to be twice as effective at depositing Reb A to the surface of the tongue as regular sweetener solution. Finally, we have demonstrated that WPI and pectin capsules can achieve a desirable pH-responsive profile for application in beverages with minimal release in acidic conditions (7.1 %) and higher release in neutral conditions (19.5 %).

1. Introduction

Sugar derivatives, polyols, and various high-intensity sweeteners have been developed to provide the desired sweetness at low or no-calorie, removing the associated health risks from excess sugar intake. Specifically, steviol extracts from *Stevia rebaudiana* Bertoni are of interest as natural high-intensity sweeteners. Stevia and its various derivatives are widely used as a sugar substitutes in medicines, foods, and beverages. Its main appeal comes from its safety and non-synthetic origin, answering the growing demand for more naturalness in the past 30 years (Battacchi, Verkerk, Pellegrini, Fogliano, & Steenbekkers, 2020; M.; Carocho, Morales, & Ferreira, 2017; Márcio Carocho, Morales, & Ferreira, 2015; Román, Sánchez-Siles, & Siegrist, 2017). Functionally, Stevia has exhibited good stability at higher temperature and over a wide variety pH conditions within food matrices. It provides good sweetening power, but there is a noticeably bitter aftertaste with a note of black licorice at higher concentrations, depending on individual sensitivity (Ahmad, Khan, Blundell, Azzopardi, & Mahomoodally, 2020; Aidoo, Depypere, Afoakwa, & Dewettinck, 2013; M.; Carocho et al., 2017).

Rebaudioside A (Reb A) is the component of Stevia extract that has a sweetening power approximately 300 times that of sucrose. While Reb A has the highest stability of the steviol glycosides (Aidoo et al., 2013), its sweetening power and stability varies with environmental conditions such as pH, matrix composition, and temperature. However, Reb A's family of sugar substitutes suffer from the lack of bulk-forming capability, a non-sugar-like sweetness profile and a bitter aftertaste beyond a certain concentration (Aidoo et al., 2013). Various attempts have been used to alleviate the bitter aftertaste and improve the sweetness potency of steviosides such as enzymatic or chemical transglycosylation (Ye et al., 2013, 2014) and hydrolysis (de Oliveira, Packer, Chimelli, & de Jesus, 2007; H.-d.; Wan, Tao, Kim, & Xia, 2012). However, these methods are costly and the improvement offered, limited.

Encapsulation has been used for taste-masking of unpleasant drugs

* Corresponding author. 243 Stocking Hall, Ithaca, NY, 14850-7201
E-mail address: Alireza@cornell.edu (A. Abbaspourrad).

https://doi.org/10.1016/j.foodhyd.2022.107657
Received 14 December 2021; Received in revised form 23 February 2022; Accepted 10 March 2022
Available online 12 March 2022
0268-005X/

and for controlled release purposes (Shah, Madan, & Agrawal, 2012). The application of this method for use with sweeteners is of great interest to the food industry. Encapsulation of aspartame and sucralose was achieved through the inclusion of the cargo within lipid coatings (Wetzel & Bell, 1998) or within biopolymer particles formed with complex coacervation (Rocha-Selmi, Bozza, Thomazini, Bolini, & Favaro-Trindade, 2013; Rocha-Selmi, Theodoro, Thomazini, Bolini, & Favaro-Trindade, 2013). These studies are geared toward the application of these materials in solid food applications such as baking or chewing gum. These applications require low solubility, low hygroscopicity and prolonged release after exposure to liquid media and are therefore not applicable to systems such as acidic beverages.

Therefore, we have chosen to fabricate nanocapsules from mucoadhesive materials through an ultrasonic process, using food grade biopolymers of hydrolyzed whey protein isolate, and pectin. We have developed a method for loading hydrophilic cargo and have encapsulated Reb A in a nanocapsule that holds and releases its cargo in response to pH changes.

2. Material and method

2.1. Materials

Thermax® 690 hydrolyzed whey protein isolate (WPI) was donated by Glanbia Nutritionals, Incorporated (Fitchburg, WI, USA) (lot# 0888321). TIC Pretested® pectin powder (low-methoxylated 35 %) and κ-carrageenan were obtained from TIC Gums, Incorporated (Belcamp, MD, US). Sodium dodecyl sulfate (SDS), and Span 80 were obtained from Sigma-Aldrich (St. Louis, MO, US). Rebaudioside A (Reb A) (≥96 % purity) was donated by The Coca-Cola Company (Atlanta, GA, US). Xanthan gum was purchased from Colony Gums (Monroe, NC, US). Corn oil (Mazola, ACH Food Companies, Incorporated, Cordova, TN, US) was purchased from a local supermarket. The gel electrophoresis reagents were purchased from Bio-Rad Laboratories (Hercules, CA, US). All water used was deionized (18.2 MΩ/cm) with a Millipore water purification system.

Thermax® 690 hydrolyzed whey protein isolate (WPI) was analyzed with SDS-PAGE (data not showed) and found to be composed majorly of peptides around <10–15 kDa range. Among them, 3 distinctive bands were shown in this region, suggesting that three population of molecular weights. However, the smear in this region suggested that a portion of the peptide did not have uniform mass which is expected of hydrolyzed protein. Peculiarly, there was a distinct sharp band around ~60 kDa that could correspond to bovine serum albumin, which somehow remained intact after the processing.

2.2. Core-shell nano-capsules synthesis

2.2.1. Ultrasonication parameters

The nano-capsule fabrication method was slightly modified from the water-in-oil emulsion interfacial polymerization process as described in our previous work to encapsulate hydrophilic cargo (Tan et al., 2019). A mixture of protein and polysaccharide was used to provide a wider variety of functional groups that can participate in crosslinking reactions (Shanshan et al., 2021).

In the encapsulation of Reb A in the model WPI-Pectin system, 4 mL of WPI (1.5 % w/v), 4 mL of pectin (1.5 % w/v), and 0.7 mL of Reb A solutions (0.8 % w/v) made up the aqueous phase. The sweetener solution was made daily to prevent precipitation due to the hydration of Reb A at the concentrations used at room temperature. For samples with protein and two polysaccharides as shell material, only 3 mL of the pectin solution was added along with 1 mL of either xanthan or κ-carrageenan (0.5 % w/v). The partial substitution of the main polysaccharide was done to probe the influence of the materials that the shell is composed of on the properties of the final capsule. Interaction between the shell materials before sonication was minimized by adjusting the pH of the WPI and pectin solutions to 6.0 with 1 M sodium hydroxide or hydrochloric acid. After gentle swirling to mix the protein and polysaccharides, the resultant liquid must not be allowed to stand in order to prevent possible aggregation. The oil phase, comprised of 20 mL of corn oil and 0.3 g of Span 80, was added to the beaker and the mixture was sonicated.

A 750 W, 20 kHz ultrasonic processor with 13 mm high-power sonic tip (VC 750, Sonics Vibra-cell, Sonics & Materials, Newtown, CT, US) was then used to prepare the emulsion from the resulting mix. The reaction beaker was immersed in an ice bath to prevent excessive heat buildup and increase the stability of radicals generated during ultrasonication. The probe head was lowered onto the interface between oil and water. The mixture was sonicated for 8 min at 300 Wcm^{-2} intensity (5s on, 2s off). The beaker was visually checked for proper immersion depth in the ice bath and swirled gently for 4 min to ensure homogeneity.

2.2.2. Capsule isolation and washing

After ultrasonication, the nanocapsules that were formed were suspended within the water/oil (W/O) emulsion. To extract them, first, the sonicated solution was centrifuged at 15,000×*g* for 15 min to separate the aqueous phase from the bulk of oil. The nanocapsule pellet forms a white gel-like clump at the bottom of the centrifugal vessel in the water phase. Due to the difficulty of completely removing the oil layer, the aqueous layer and solid pellet were pipetted into a fresh container. The mixture was centrifuged again at 15,000×*g* for 15 min. The supernatant was decanted to yield a crude capsule, in the sense that some oil residue remained. Depending on the downstream experiments, the nanocapsules could be further purified with a washing step or resuspended and used immediately in the release study.

The washing protocol included resuspending the capsule pellet in 5 mL of clean 60 mM citrate buffer (pH 6.0) and centrifuging at 15,000×*g* for 15 min. The removal of supernatant then completed one wash cycle. This procedure was done twice to ensure removal of the oil phase. The capsules with minimum corn oil residue were then suspended in an appropriate buffer for downstream testing and stored at 4 °C in the dark as appropriate.

2.3. Scanning electron microscopy (SEM)

To observe the morphology of the capsule on the nanometer scale and to ensure proper formation, SEM was used. The samples were prepared using the method outlined above with two wash cycles. The nanocapsules were resuspended in 60 mM citrate buffer (pH 6.0), dripped onto an SEM plate with carbon conductive tab (Electron Microscopy Science Inc, Hatfield, PA, USA) and dried overnight under vacuum. The morphology and structure of the nanoparticles were observed using a Zeiss Gemini 500 field emission scanning electron microscope (FE-SEM, Germany), with 20 μm aperture size, 1.1 nm probe size, and 1.00 kV and 37 pA current. The SEM samples were coated with a 15 nm layer of Au–Pd *via* Denton Desk V sputter coater (Moorestown, NJ USA) before the SEM test.

2.4. Hydrodynamic diameter Z-average and ζ-potential measurement

To evaluate the stability of the nanocapsule within the model beverage condition, Zetasizer Nano-ZS90 (Malvern Instrument Ltd., UK) was used to measure the hydrodynamic particle size and ζ-potential through dynamic light scattering (DLS). For Z-average measurement, the nano-capsules pellet after the washing process was dispersed in 5 mL of 10 mM citrate buffer (pH 6.0) as a stock suspension. A 50 μL aliquot was then taken and diluted with 950 μL of the same buffer in a polymer cuvette and measured for the Z-average. The cell temperature was set to 25 °C and outfitted with a He/Ne laser (λ = 633 nm) set at the scattering angle of 90°. For ζ-potential measurement, the 100 μL stock capsule suspension was diluted with 900 μL of 60 mM citrate buffer (pH 6.0) and

loaded into a disposable folded capillary cell (DTS1070) for analysis. The software utilized the Smoluchowski model for the calculation.

2.5. Thermogravimetric analysis (TGA)

To determine the difference in thermal stability, and asses the physical properties of the shell materials before and after fabrication into nanocapsules, TGA was employed. Approximately 5 mg of the lyophilized samples were loaded onto the platinum pan, which was then placed in the autosampler of the thermogravimetric analyzer (TGA Q500, TA Instrument, New Castle, DE, USA). The pan was lowered into a chamber with flowing nitrogen gas at 60 mL/min and heated from room temperature to 450 °C at the rate of 10 °C/min. The first derivative of percent mass loss over temperature was plotted against heating temperature.

2.6. High-resolution X-ray Photoelectron Spectroscopy (XPS)

To explain the nature of the difference in the nanocapsules before and after ultrasonication, High-res XPS was used to analyze the change in chemical bonding induced during processing. The changes in functional groups in the shell materials can provide confirmation of the nature of the interaction between the biopolymers. XPS spectroscopy was performed with Scienta Omicron ESCA-2SR with operating pressure $\sim 1 \times 10^{-9}$ mBar. Monochromatic Al Kα X-rays (1486.6 eV) were generated at 300 W (15 kV; 20 mA). Analysis spot size was 2 mm in diameter with a 0° photoemission angle and a source to analyzer angle of 54.7°. A hemispherical analyzer determined electron kinetic energy using a pass energy of 200 eV for survey scans and 50 eV for high resolution scans. A flood gun was used for charge neutralization of non-conductive samples.

2.7. Encapsulation efficiency and loading content

Encapsulation efficiency is used to evaluate the entrapment effectiveness of the ultrasonic encapsulation process. This percentage indicates the amount of the cargo that has been incorporated into the nanocapsule. A higher percentage indicates a more efficient, and thus more economically viable, process.

The measurement was conducted via an indirect method. The Reb A left unencapsulated after the encapsulation process was quantified and then compared to the initial quantity. The crude nanocapsule sample is collected before the final washing step and a 500 μL supernatant aliquot was transferred to a 30 kDa centrifugal filter (Amicon® Ultra-0.5, MilliporeSigma) and spun at 14,000×*g* for 15 min. Then, 120 μL of the permeate was diluted with 875 μL Milli-Q water in a glass vial for LC-MS analysis. This sample was used to evaluate the amount of Reb A that remained after encapsulation and thus the encapsulation efficiency of the system could be calculated.

Samples were run on an Agilent 1100 HPLC coupled to a Thermo LTQ MSn ion trap with an ESI ion source. The isocratic mobile phase consisted of 0.01 % (v/v) formic acid and acetonitrile in a ratio of 75:25, respectively, at a flow rate of 0.6 mL per minute. The HPLC column used was a Phenomenex Luna Omega Polar C18 3 μM 4.6 mm × 100 mm. The column was held at room temperature and not heated. The injection volume was 10 μL for all samples. The ion source was operated in negative ion mode using the following parameters: Sheath gas flow rate 50, Aux gas flow rate 15 (arbitrary unit based of MS software Xcalibur™ by Thermo Scientific), spray voltage 5.0 kV, capillary temperature 350 °C, capillary voltage 35.0 V, and tube lens 110 V. Total run time for all samples and scan types was 30 min. Samples were run using selected reaction monitoring (SRM) scan mode mass transition monitored was 966.3 m/z to 804.3 m/z with a mass window of 5 m/z. Rebaudioside M was used as an internal standard to monitor and correct for any fluctuation in the peak area of Reb A due to sampling matrix effects. Equation (1) shows the encapsulation efficiency calculation from the Reb A before and after ultrasonication process.

$$Encapsulation\ efficiency\ (\%) = \frac{total\ RebA - unencapsulated\ RebA}{total\ Reb\ A} \times 100\% \quad (1)$$

Loading content was another parameter investigated as it relates the proportion of cargo to shell material mass. This impacts the dosage of the nanocapsule in beverage applications, allowing for the calculation of the powder necessary to achieve equivalent mass of sweetener. The washed nanocapsule pellet was cooled to −20 °C for 5 h and then lyophilized for 24 h before weighing on a balance. The result from Reb A quantification above and the measurement gathered here were used in the subsequent calculation below. Equation (2) shows the percent of shell material out of the total mass added that was converted into nanocapsules, while equation (3) shows the loading content calculation.

$$Nanocapsule\ yield\ (\%) = \frac{total\ shell\ material - nanocapsule\ mass}{total\ shell\ material} \times 100\% \quad (2)$$

$$Loading\ content\ (\%) = \frac{mass\ encapsulated\ RebA}{nanocapsule\ mass} \times 100\% \quad (3)$$

2.8. Quartz crystal microbalance with dissipation monitoring (QCM-D)

A Q-Sense Analyzer quad-module system (Biolin Scientific, Gothenburg, Sweden) equipped with a gold sensor (QSX 301) was used in this study. - The sensor was cleaned in a mixture of Milli-Q water, ammonia, hydrogen peroxide (5:1:1) at 75 °C for 5 min, rinsed and subjected to UV-Ozone treatment for 10 min. Then, it was rinsed with Milli-Q water, dried with nitrogen gas, and treated with UV-Ozone for 10 min.

Washed nanocapsules were prepared according to Section 2.3 and dispersed in 100 mL of 10 mM citrate buffer at pH 3.2 to simulate the beverage condition. The control used was 100 mL of a 20 mg/L Reb A solution in the same buffer. A Four-channel QCM-D instrument was used to simultaneously process three replicates of the capsule sample along with one control.

At the flow rate of 0.3 mL/min, mucin (0.1 % in 10 mM phosphate, pH 7.0) was simultaneously injected into the instrument. When the frequency shift stabilized for 3 min, the phosphate buffer at pH 7.0 was injected to wash out the loosely bound mucin layer on the gold sensor. To account for the effect of compaction due to pH change, a pH 3.2 citrate buffer was injected to equilibrize the layer before sample injection. After the frequency shift stabilized, nanocapsule and Reb A samples are injected into the chamber. For the nanocapsule sample, each of the three cells is allotted 33 mL of suspension. When the curve stabilized, the final wash was done with pH 3.2 buffer to wash off any loosely bound nanocapsule or Reb A.

2.9. Two hour release study

After determining whether the nanocapsule retained its mucoadhesivity, it was important to confirm that the release profile of the nanocapsule matched our goal. Specifically, for acidic beverage applications, that the nanocapsule should selectively release its cargo in the near neutral pH of oral cavity and it should retain its cargo effectively at low pH. For this, we conducted a 2-h release study. Since the target site was the oral cavity and most food and beverages pass through within a minute, 2 h was considered suitably long to evaluate any possible effect on the palate.

The nanocapsules were prepared as per the procedure in Section 2.3. However, during the washing step, the crude capsule was suspended in 5 mL clean 60 mM citrate buffer (pH 6.0) and centrifuged at 15,000×*g* for 5 min. The shortened time was to minimize any possible cargo release. The supernatant and oil residue were removed as cleanly as possible.

The nanocapsule pellet, after the washing process, was dispersed in 10 mL of 10 mM citrate buffer (pH 3.2 or 6.0). The suspension was transferred to a centrifuge tube, placed upon a shaker, and shaken gently at room temperature. Then 500 μL aliquots were taken at 0, 30, 60, 90, and 120 min and added to 30 kDa centrifugal tubes and spun at 14,000×*g* for 15 min to remove the nanocapsule particles. The concentration of Reb A in the permeate was quantified with LC-MS. The cumulative release was calculated as followed.

$$Cumulative\ release\ (\%) = \frac{mass\ of\ free\ RebA}{mass\ of\ initial\ encapsulated\ RebA} \times 100\%$$

Each treatment of shell material system and pH was done in triplicate on the same day to minimize day-to-day variation.

3. Results and discussion

The goal for this study is to develop a mucoadhesive, pH-responsive nanocapsule for the transport and delivery of Reb A. We have successfully prepared and isolated nanocapsules loaded with Reb A and investigated its physical and chemical properties. Specifically, because the target application is in beverages, the nanocapsule must be able to contain the cargo at low pH, and be soluble or at least reasonably capable of being suspended in a liquid. After this confirmation, we ensured that the capsule retained its ability to attach itself to the mucin layer. Finally, we confirmed that the release profile of the capsule matched well with our target beverage application, namely releasing the cargo in near neutral solution, while retaining Reb A in a low pH environment.

3.1. Nanocapsule characterization

After synthesis and isolation of the nanocapsules, we confirmed that the collected nanocapsule pellet contained the desired Reb A. The morphology and hydrodynamic properties and viability of the nanocapsules were assessed in the targeted medium. Specifically, we inspected the shell of the capsule for successful formation and that it completely encased the internal environment separately from the outside environment. Further, we employed various techniques like TGA and High-res XPS to understand the nature of the chemical interaction between biopolymers induced by high energy ultrasonication.

3.1.1. SEM

Ultrasonic fabrication of nanocapsules relies on cavitation to form the aqueous droplet and the radical generation from water sonolysis to crosslink the protein-polysaccharide shell (Y. Han et al., 2010; K. Suslick, Grinstaff, Kolbeck, & Wong, 1994; K. S. Suslick et al., 1999; K. S. Suslick & Grinstaff, 1990; Tzhayik, Cavaco-Paulo, & Gedanken, 2012). Scanning electron microscopy (SEM) image **A3** in Fig. 1 shows the successful formation of nanocapsules from WPI-Pectin. Morphologically, a large proportion of the nanocapsules have a relatively smooth surface but are unevenly shaped. The structure appeared completely encased without any obvious cracks, suggesting isolation of internal cargo from the exterior environment.

This was promising in terms of the cargo retention. The nanocapsules also had a large distribution of particle sizes from a nm range up to slightly over μm. This was somewhat unexpected since the model method that this paper was based upon achieved relatively monodisperse particles (Suslick et al., 1994) used for anthocyanin encapsulation (Tan et al., 2019). The polydispersity suggested that the size of the emulsion droplets formed by the cavitation was not uniformed. This could be the result of the intrinsic property of material used in this study, like the large molecular weight disparity between hydrolyzed whey protein and pectin, or the inadequate acoustic treatment intensity to yield a uniform particle size.

Rarely, large particles were observed within the WPI-Pectin sample as seen in images **A1** and **A2** in Fig. 1. A crack can be seen on the surface in image **A1**, possibly due to the high vacuum required for SEM sample preparation, incomplete particle formation, or the start of shell material disassembly. This suggests that larger nanocapsules may be inherently weaker and more susceptible to damage, thus measures should be developed to standardize and lower the particle size. Further optimization could be made to the batch volume and sonication intensity (Yongsheng Han, Radziuk, Shchukin, & Moehwald, 2008).

The substitution of a small amount of pectin with other polysaccharides resulted in particles with more irregular surfaces, suggesting tangible impact on the capsule formation. In particular, the addition of κ-Carrageenan resulted in a capsule with a bumpy or jagged surface, no longer resembling a spherical shape (Fig. 1 C1 and C3). This could be explained by the larger molecular mass of the polysaccharides or the disruption in the structure caused by a mixture of different polysaccharides. It is noteworthy that a difference in morphology can be

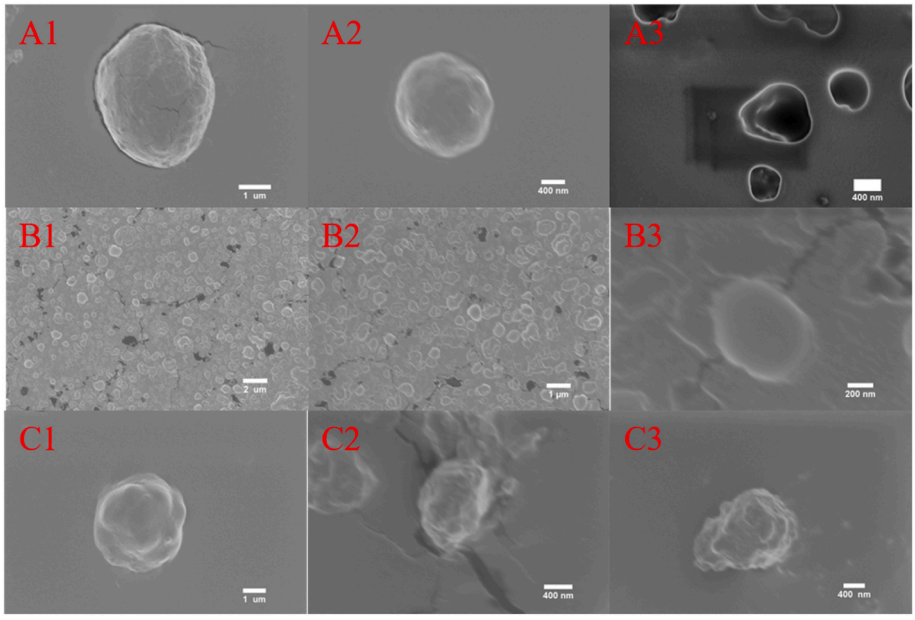

Fig. 1. Morphology of core-shell nanocapsule fashioned from (A1-3) WPI-Pectin, (B1-3) WPI-Pectin-Xanthan, and (C1-3) WPI-Pectin- κ-Carrageenan, loaded with Reb A as shown with SEM.

observed even with a minute amount of xanthan and κ-carrageenan (0.06 % w/v), suggesting that their presence in the mixture could have a significant impact on the morphology of the fabricated capsules.

3.1.2. Hydrodynamic diameter Z-average and ζ-potential

After understanding the morphology of the capsule, we characterized the parameters of the nanocapsules involving their stability in beverages, namely particle size and ζ-potential. A 10 mM citrate buffer was selected to suspend the capsule because it is the system most commonly used in the beverage industry. However, this buffer system depresses the WPI ζ-potential significantly, thus it could also negatively affect the nanoparticles derived from it.

In this buffer, nanocapsules derived from hydrolyzed WPI and pectin had enough surface charge to be considered metastable in solution. We compared the different formulations of nanocapusles and found that their ζ-potentials were not significantly different (Fig. 2). The ζ-potentials range is small, between −18.8 mV and −21.7 mV. This indicates that they could remain stable in solution for a few hours without precipitating at room temperature at a pH of 6.0. The average particle size of the nanocapsules was within the nanometer range (400 nm) and did not differ significantly between treatments. This is on the smaller side of the range achieved by other studies (0.100 μm–80 μm) (Yongsheng Han et al., 2008). This could possibly be the result of biosurfactant quality (Hou et al., 2019) and compatibility of Reb A with protein-based emulsion (Z.-L. Wan, Wang, Yang, Wang, & Wang, 2016). The nanocapsules exhibited large size distribution (polydispersity index (PDI) > 0.2). The main size populations were bimodal, centered around 200–400 nm and 1 μm.

While the inclusion of xanthan or κ-carrageenan affects the capsule morphology, there was no significant difference in terms of zeta-potential, size, and PDI, between the WPI-pectin system and the systems incorporating the second polysaccharide. This was to be expected given the relatively small amount of xanthan or κ-carrageenan included in the reaction mixture.

3.1.3. Thermal gravimetric analysis (TGA)

The TGA peak profile of the mixture of hydrolyzed WPI and pectin (green) corresponded roughly to the curve shape of the substituent materials (grey and red) at around 300 °C, 250 °C, and 200 °C, respectively (Fig. 3A). However, after being fabricated into a nanocapsule through ultrasonication (yellow), the three peaks of the physical mixture merged into one broad peak centered around 300 °C, completely distinct from the other sample. This suggests that the sonication process caused a significant change in the physical property that distinguished the sonicated sample from the simple solution mixture, suggesting possible crosslinking of the shell material. The formation of strong covalent bonds was the basis for good retention for the cargo within the capsule, thus making nanocapsules produced by ultrasonication promising.

While the addition of the second polysaccharide did not significantly alter the morphology and hydrodynamic parameters of the particle, the difference in TGA peak shape provides evidence for their incorporation in the nanocapsule formation step (Fig. 3B). Even with a modest addition of around 0.06 % w/v of the reaction mixture, capsules with either xanthan or κ-Carrageenan showed distinct reaction profiles.

In the SEM and Zetasizer analyses, xanthan or κ-carrageenan only appeared to modify the morphology of the capsule without significantly altering the hydrodynamic properties of the nanocapsules, providing no convincing argument to choose one system over another. However, there was a noticeable difference in thermal stability, thus the physical property of these systems suggested that their release profile might also be distinct.

3.1.4. High-res X-ray Photoelectron Spectroscopy (XPS)

High-resolution X-ray Photoelectron Spectroscopy (XPS) was used to further characterize the nature of the crosslinking of the nanocapsule shells. Images **A1-A3** in Fig. 4 show the XPS spectra of WPI, the WPI pectin mixture, and the sonicated WPI-pectin mixture. The N 1s spectra of the protein and physical mixture appeared very similar. This was expected since pectin does not have an appreciable amount of nitrogen groups. Interestingly, although the level of amide bonds remained similar (Fig. 4B) mixing protein solution with pectin partially protonated some of the amine groups, abundant in the N-terminus of hydrolyzed protein, into ammonium ions. However, the spectra of the mixture before and after ultrasonication shows a stark, clear reduction in the intensity of the peak (~397.7 eV) associated with an amine. The amide peak (~400 eV) of the sonicated mixture also increased dramatically while shifting slightly to the left. The ammonium peak disappears entirely into the baseline. This observation suggested the successful formation of an amide bond from the $–NH_2$ group of the protein and –COOH group of both the protein and the pectin via ultrasonication. Given the known starting reactant of bond formation, it is possible that the degree of crosslinking could be modulated by varying the amount of N-terminal or amine-bearing amino acid residues within the protein. By integrating the area under the curve and adjusting for the XPS baseline with the Tougaard model, the degree of amide crosslinking was calculated to be approximately 62.0 %. This amide bond formation was also observed in a similar study using bovine serum albumin as shell material (Tan et al., 2019), which was suggested to be the basis for reducing capsule porosity, improving the chemical stability and cargo retention of the ultrasonicated protein polysaccharide system.

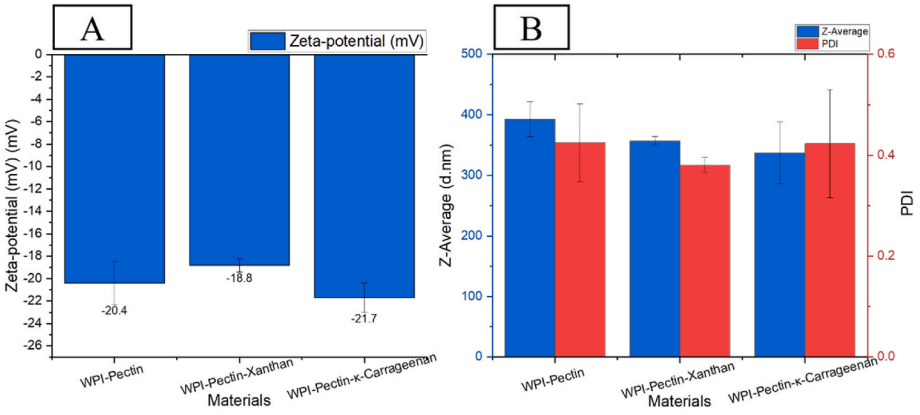

Fig. 2. (A) ζ-potential, (B) Z-average and Polydispersity Index (PDI) of WPI-Pectin nanocapsules and its derivatives system in 10 mM citrate buffer pH 6.0. There was no statistical significance between ζ-potential (F_2,9 = 3.322, p = 0.089), Z-average (F_2,9 = 2.624, p = 0.141), and PDI (F_2,9 = 0.352, p = 0.715).

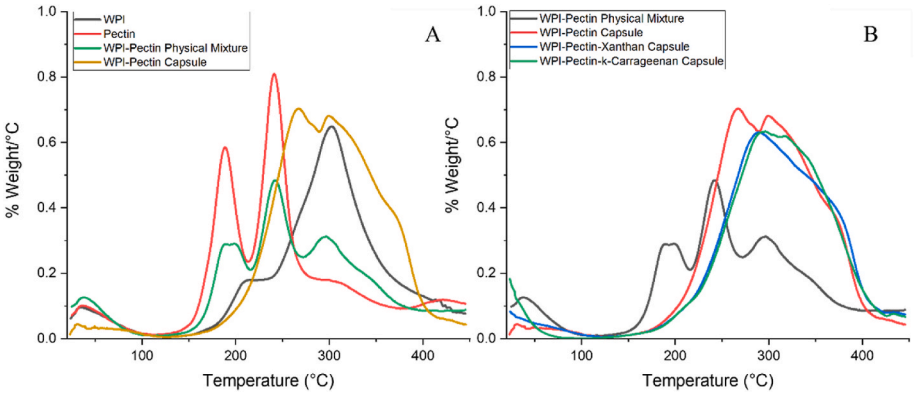

Fig. 3. First derivative thermogravimetric curve of (A) WPI-Pectin interaction (B) WPI-Pectin capsule with polysaccharide additive.

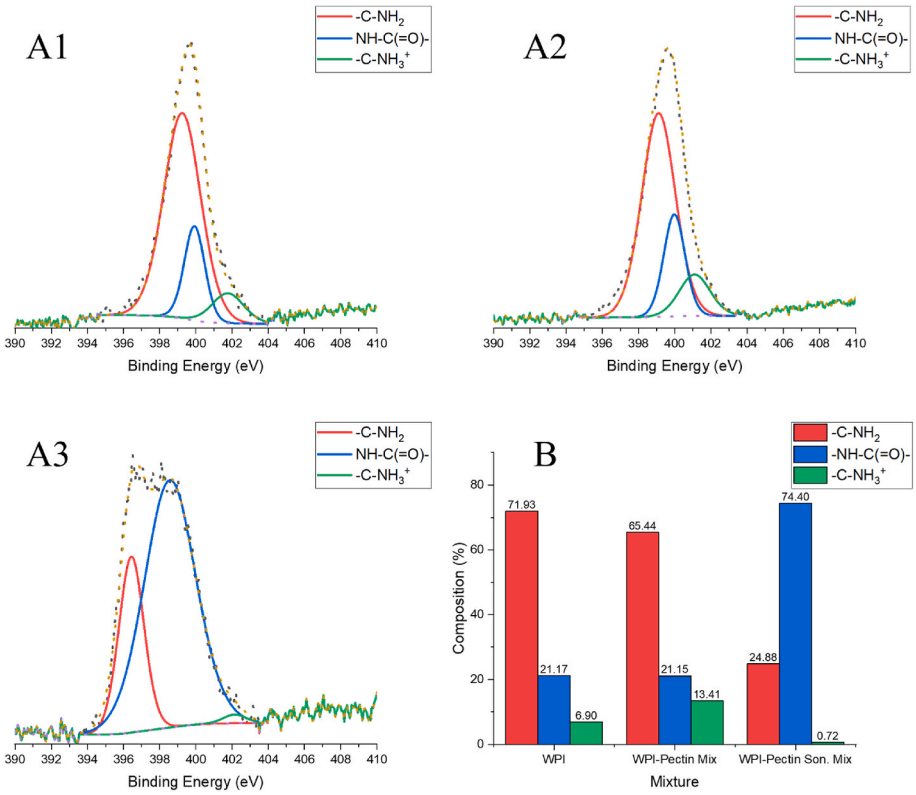

Fig. 4. N 1s High-resolution XPS spectra of (A1) WPI, (A2) physical mixture of WPI-Pectin, and (A3) sonicated mixture of WPI-Pectin. (B) Composition of nitrogen bond.

3.2. Mucoadhesion

To confirm whether the fabricated nanocapsule retained the high mucoadhesivity attributed to WPI, and if its mucoadhesivity increases the delivery of the sweetener, QCM-D was used.

QCM-D is a real-time and non-destructive monitoring technique that can detect nanoscale interactions, such as the nanocapsule attachment to a mucin layer used to simulate the mucous membrane of the tongue (Wang, Dadmohammadi, Jaiswal, & Abbaspourrad, 2020; Yan et al., 2021). This helped evaluate the nanocapsule efficiency ability to deliver the cargo. By comparing the equivalent mass of Reb A deposited onto the mucin, it was possible to determine whether the encapsulation in WPI and pectin increased the effectiveness of delivering the sweetener to the surface of the tongue.

As stated in the goal of this research, the nanocapsule shell encasing the sweetener must be mucoadhesive to increase the length of exposure to the tongue surface. While WPI was known for its astringency and mucoadhesivity, its interaction with pectin and Reb A under ultrasonic conditions could alter the structure significantly enough to compromise this quality. Secondly, we needed to confirm whether this mucoadhesivity allowed better deposition of sweetener molecule onto the mucin layer surpassing the unmodified Reb A solutions. If more nanocapsules adhere to the mucin layer and release their cargo, then less sweetener will be needed in the bulk phase overall, delivering the desired level of sweetness with less sweetener.

The nanocapsule suspension deposited comparatively more total material on the gold sensor when compared to 20 mg/L Reb A solution under the same conditions (not shown). Even after adjusting for the average Reb A loading content of 5.75 % (Fig. 5), there was still a clear disparity between the Reb A deposition on the sensor between the capsule and pure solution (Fig. 5B). This can be explained due to the strong protein-protein interaction between the existing mucin layer, and

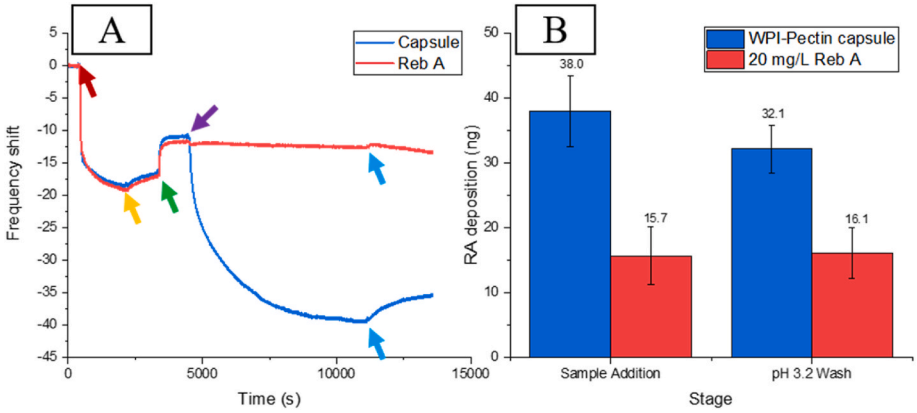

Fig. 5. (A) Frequency shift overtime of the quartz sensor, arrows indicate the different reaction events: the start of mucin (red), pH 7.0 buffer (yellow), pH 3.0 buffer (green), sample (purple), and the final pH 3.0 buffer wash (light blue), respectively. (B) Reb A deposited on the sensor, calculated from the mucin layer after pH 3.0 as a baseline. The capsule demonstrates significantly high Reb A deposition during both sample addition (t_4 = 7.851, p = 0.001) and after wash (t_4 = 6.335, p = 0.003). (For interpretation of the references to colour in this figure legend, the reader is referred to the Web version of this article.)

the capsule suspension flowing across it. Comparatively, pure Reb A had little means to attach to the mucin other than physical entrapment within the fibrous structure, which was unlikely due to the compaction caused in acidic conditions.

After the final pH 3.2 wash, the capsule layer lost some mass, hence the reduction in Reb A deposition. This was attributed to the removal of loosely bound WPI-pectin capsules from the mucin. This behavior was similar to the one observed after washing the initial mucin layer with pH 7.0 phosphate buffer (yellow arrow). However, in pure Reb A solution, the final buffer wash did not cause appreciable change in mass. This suggests that the Reb A molecules were more tightly bound to the mucin layer. However, the disparity in Reb A mass deposited between the capsule and the control during the sample addition phase still could not be dismissed. Therefore, it could be concluded that the capsule retained the mucoadhesive property of its constituent WPI.

Our second goal was to evaluate the intensity of the sweetness perceived by the tongue. For this purpose, the encapsulation platform must be capable of releasing its cargo, the taste compound, at the site of action. This can be tested indirectly and directly through release profile and sensory evaluation, respectively. We report here the release profile data for our system. The sensory evaluation, however, was deemed outside the scope of this study and will be conducted at a later time.

3.3. Release profile over 2 h

We hypothesized that the fabrication of a delivery vehicle from multiple polymers would confer added functionality in such a way that benefits the intended application in an acidic beverage application. In addition to improving the material efficiency of the encapsulation process, thus increasing the economic viability, the alteration of nanocapsule shell material composition should also modulate the release profile of the sweetener cargo. In particular, we were interested in the effect of pH on cargo retention. For application in an acidic beverage, it would be ideal for greater retention at low pH, simulating storage in the beverage, and high release at the near neutral pH of the target site in the oral cavity. Furthermore, the release should also be rapid to prevent the unpleasant delayed onset of sweetness, noted as a defect in many high-intensity sweeteners.

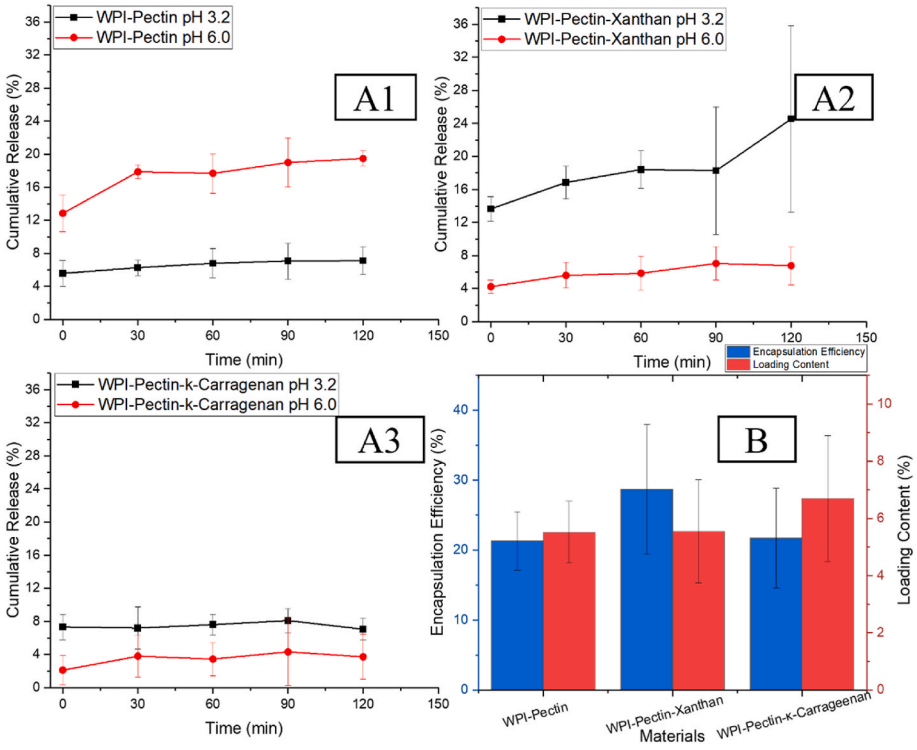

Fig. 6. The release profile of Reb A from: WPI-Pectin (**A1**) – interaction between pH and time (F_4,29 = 0.897, p = 0.484) and main effect of time were not statistically significant (F_4,29 = 1.849, p = 0.158), but the main effect of pH was statistically significant (F_4,29 = 136.59, p < 0.0001), WPI-Pectin-Xanthan (**A2**) – interaction between pH and time (F_4,24 = 0.783, p = 0.554) and main effect of time were not statistically significant (F_4,24 = 1.839, p = 0.174), but the main effect of pH was statistically significant (F_4,24 = 60.10, p < 0.0001), and WPI-Pectin-κ-Carrageenan Xanthan (**A3**) – interaction between pH and time (F_4,24 = 0.160, p = 0.955) and main effect of time were not statistically significant (F_4,24 = 0.308, p = 0.868), but the main effect of pH was statistically significant (F_4,24 = 21.76, p = 0.0003) – at pH 3.2 (black) and pH 6.0 (red) in 10 mM citrate buffer. (**B**) The encapsulation efficiency and loading content of each system. There was no significant difference between treatments in encapsulation efficiency (F_2,14 = 1.817, p = 0.205) and loading content (F_2,14 = 0.606, p = 0.561). (For interpretation of the references to colour in this figure legend, the reader is referred to the Web version of this article.)

The addition of secondary polysaccharide did not have an impact on the encapsulation efficiency (Fig. 6B). Both xanthan and κ-carrageenan also exacerbated the variability of the encapsulation efficiency between different batches. On the other hand, the second polysaccharide allowed for a slight adjustment of yield and loading content. An increase in capsule mass was observed in the sample with xanthan, while the encapsulated Reb A remained the same.

This meant that the ratio between Reb A and shell material mass in the capsule decreased. On the other hand, κ-carrageenan yielded fewer nanocapsules while maintaining cargo levels, thus a higher loading content. This is a beneficial feature in the beverage industry since it would require less nanocapsule addition to achieve the same mass of sweetener.

The WPI-Pectin capsule in 10 mM citrate buffer system at pH 3.2 released less than 6.3% of its encapsulated Reb A in 30 min and about 7.1 % over the entire 3 h (Fig. 6 A1). This suggested that the capsules fashioned with this formulation boasted good retention in the expected storage pH and ionic strength: a desirable quality to minimize leeching of sweeteners from the delivery vehicle during storage. Conversely the capsules suspended in pH 6.0 buffer were released almost three times more (~18 %) in 30 min, after which cargo release plateaued at 19 %. The release profile matched the characteristics desired for the intended application in the acidic beverage: retention of cargo at low pH and release of cargo at near neutral pH.

Incorporation of 4.5 % of xanthan into the shell material mass, drastically altered the release characteristics of the capsules. The addition of xanthan reversed the trend of the original WPI pectin system and produced a capsule with great retention at near-neutral pH, plateauing at 6.8 % after 2 h. There was also a rapid release of cargo after the exposure to the buffer since the starting data points for pH 3.2 reproducibly yielded a large amount of Reb A than at pH 6 (Fig. 6 A2). Although unfit for the application in beverages, the system may find uses in another fields of application.

While showing slightly better loading content, suitable for beverage application, the κ-carrageenan release profile did not adequately show pH responsiveness. The value fluctuated throughout 2 h, with large variations between true replicates. Although there was a statistically significance between pH, suggesting responsiveness to the environment, the effect size was too small and the capsule was more partial toward release in acidic conditions. We attribute some of this fluctuation to the non-homogeneous nature of the nanocapsules produced by our benchtop, wand ultrasound.

Overall, the WPI-Pectin capsule met the most criteria sought for the ideal encapsulation platform, but there were still many limitations, namely the maximum release and fabrication reliability. In the condition in which the capsules were meant to release the cargo, the maximum release of ~19 % is an inefficient use of sweetener. However, the platform demonstrated itself to be very tunable by adding different polysaccharides into the shell material mix. Further study is warranted to find the combination with the most desirable characteristics. Secondly, the fabrication reliability needed improvement. The large standard deviation of the release data was the result of the average release profiles of different batch of capsules under one treatment. The variability across batch can be detrimental and had to be eliminated before upscaling.

4. Conclusion

From this study, the modified ultrasonic crosslinking method was capable of fabricating nanocapsules from proteins and polysaccharides and encapsulating Reb A. The cavitation did not alter or denatured the protein enough and its mucoadhesivity was retained, offering an avenue of research into other material with strong interaction with the mucin layer. Doping the reaction mixture with different polysaccharides had a profound impact on the release profile of the capsule, suggesting that it can be used to modulate the pH responsiveness of nanocapsules made from different materials. We found that WPI-Pectin was the most suitable of all the protein-polysaccharide combinations tested, yielding nanocapsules that demonstrated a suitable pH-responsiveness profile for use in beverage applications with minimal release in acidic conditions (7.1 %) and higher release in neutral conditions (19.5 %), however, the challenge of modest encapsulation efficiency remains.

While it is reasonable to assume that the concentration of the taste molecule corresponds to the intensity of the perception, many factors in food settings, such as matrix composition, were neglected in this study. Therefore, while our release profiles provide some information about the perception profile, the method we used is an indirect method and therefore limited. Further, the unpleasant aftertaste of Reb A associated with usage at high concentration also was not evaluated. Therefore, further sensory studies are needed to evaluate the effectiveness of this encapsulation platform as a sweetening enhancer and delivery method. The ultrasonic process however proved that we could encapsulate Reb A in WPI with a pH responsive release profile while retaining the proteins mucoadhesivity.

Author CRediT statement

B.Pomon: conceptualization, data curation, formal analysis, investigation, writing original draft, review & editing**. S.M. Davachi, P. Li, M. Arshadi, S.S. Madarshahian**: data curation, investigation, writing – review & editing. **Y. Dadmohammadi**: conceptualization, supervision, investigation, writing – review & editing. **C. Tan**: methodology. **R.D. Woodyer, R.M.Kriegel, C.P. Mercogliano**: conceptualization, resources, funding acquisition, writing – review & editing. **A. Abbaspourrad**: conceptualization, funding acquisition, project administration, resources, supervision, writing – review & editing.

Declaration of competing interest

The authors declare the following financial interests/personal relationships which may be considered as potential competing interests: Alireza Abbaspourrad reports financial support was provided by The Coca Cola Company.

Acknowledgment

We thank the Cornell Center for Materials Research (CCMR) for the use of their facilities. CCMR facilities are supported by the National Science Foundation under award number DMR-1719875. We thank The Coca-Cola Company for their continued support of academic and research pursuits. The authors would like to thank Nanoscience and Biolin Scientific for providing the QCM-D equipment, the QSence Analyzer, and for their generous technical support. We also thank Bing Yan for valuable input throughout the entire process.

References

Ahmad, J., Khan, I., Blundell, R., Azzopardi, J., & Mahomoodally, M. F. (2020). Stevia rebaudiana Bertoni.: An updated review of its health benefits, industrial applications and safety. *Trends in Food Science & Technology, 100*, 177–189.

Aidoo, R. P., Depypere, F., Afoakwa, E. O., & Dewettinck, K. (2013). Industrial manufacture of sugar-free chocolates – applicability of alternative sweeteners and carbohydrate polymers as raw materials in product development. *Trends in Food Science & Technology, 32*(2), 84–96.

Battacchi, D., Verkerk, R., Pellegrini, N., Fogliano, V., & Steenbekkers, B. (2020). The state of the art of food ingredients' naturalness evaluation: A review of proposed approaches and their relation with consumer trends. *Trends in Food Science & Technology, 106*, 434–444.

Carocho, M., Morales, P., & Ferreira, I. C. F. R. (2015). Natural food additives: Quo vadis? *Trends in Food Science & Technology, 45*(2), 284–295.

Carocho, M., Morales, P., & Ferreira, I. (2017). Sweeteners as food additives in the XXI century: A review of what is known, and what is to come. *Food and Chemical Toxicology, 107*(Pt A), 302–317.

Han, Y., Radziuk, D., Shchukin, D., & Moehwald, H. (2008). Stability and size dependence of protein microspheres prepared by ultrasonication. *Journal of Materials Chemistry, 18*(42).

Han, Y., Shchukin, D., Yang, J., Simon, C. R., Fuchs, H., & Mohwald, H. (2010). Biocompatible protein nanocontainers for controlled drugs release. *ACS Nano, 4*(5), 2838–2844.

Hou, Y., Wang, H., Zhang, F., Sun, F., Xin, M., Li, M., et al. (2019). Novel self-nanomicellizing solid dispersion based on rebaudioside A: A potential nanoplatform for oral delivery of curcumin. *International Journal of Nanomedicine, 14*, 557–571.

de Oliveira, B. H., Packer, J. F., Chimelli, M., & de Jesus, D. A. (2007). Enzymatic modification of stevioside by cell-free extract of Gibberella fujikuroi. *Journal of Biotechnology, 131*(1), 92–96.

Rocha-Selmi, G. A., Bozza, F. T., Thomazini, M., Bolini, H. M. A., & Favaro-Trindade, C. S. (2013). Microencapsulation of aspartame by double emulsion followed by complex coacervation to provide protection and prolong sweetness. *Food Chemistry, 139*(1–4), 72–78.

Rocha-Selmi, G. A., Theodoro, A. C., Thomazini, M., Bolini, H. M. A., & Favaro-Trindade, C. S. (2013). Double emulsion stage prior to complex coacervation process for microencapsulation of sweetener sucralose. *Journal of Food Engineering, 119*(1), 28–32.

Román, S., Sánchez-Siles, L. M., & Siegrist, M. (2017). The importance of food naturalness for consumers: Results of a systematic review. *Trends in Food Science & Technology, 67*, 44–57.

Shah, S., Madan, S., & Agrawal, S. S. (2012). Formulation and evaluation of microsphere based oro dispersible tablets of itopride hcl. *Daru Journal of Pharmaceutical Sciences, 20*.

Suslick, K. S., BlakePerutz, J. R., Didenko, Y., Fang, M. M., Hyeon, T., Kolbeck, K. J., et al. (1999). Acoustic cavitation and its chemical consequences. *Philosophical Transactions of the Royal Society of London,Series A: Mathematical, Physical and Engineering Sciences, 357*(1751), 335–353.

Suslick, K. S., & Grinstaff, M. W. (1990). Protein microencapsulation of nonaqueous liquids. *Journal of the American Chemical Society, 112*(21), 7807–7809.

Shanshan, W., Meigui, H., Chunyang, L., Zhi, C., Li, C., Wuyang, H., et al. (2021). Fabrication of ovalbumin-burdock polysaccharide complexes as interfacial stabilizers for nanostructured lipid carriers: Effects of high-intensity ultrasound treatment. *Food Hydrocolloids, 111*. https://doi.org/10.1016/j.foodhyd.2021.107172

Suslick, K., Grinstaff, M., Kolbeck, K., & Wong, M. (1994). Characterization of sonochemically prepared proteinaceous microspheres. *Ultrasonics Sonochemistry, 1*(1), S65–S68.

Tan, C., Arshadi, M., Lee, M. C., Godec, M., Azizi, M., Yan, B., et al. (2019). A robust aqueous core-shell-shell coconut-like nanostructure for stimuli-responsive delivery of hydrophilic cargo. *ACS Nano, 13*(8), 9016–9027.

Tzhayik, O., Cavaco-Paulo, A., & Gedanken, A. (2012). Fragrance release profile from sonochemically prepared protein microsphere containers. *Ultrasonics Sonochemistry, 19*(4), 858–863.

Wang, J., Dadmohammadi, Y., Jaiswal, A., & Abbaspourrad, A. (2020). Investigation of the interaction between N-Acetyl-l-Cysteine and ovalbumin by spectroscopic studies, molecular docking simulation, and real-time quartz crystal microbalance with dissipation. *Journal of Agricultural and Food Chemistry, 68*(37), 10184–10190.

Wan, H.-d., Tao, G.-j., Kim, D., & Xia, Y.-m. (2012). Enzymatic preparation of a natural sweetener rubusoside from specific hydrolysis of stevioside with β-galactosidase from Aspergillus sp. *Journal of Molecular Catalysis B: Enzymatic, 82*, 12–17.

Wan, Z.-L., Wang, L.-Y., Yang, X.-Q., Wang, J.-M., & Wang, L.-J. (2016). Controlled formation and stabilization of nanosized colloidal suspensions by combination of soy protein and biosurfactant stevioside as stabilizers. *Food Hydrocolloids, 52*, 317–328.

Wetzel, C. R., & Bell, L. N. (1998). Chemical stability of encapsulated aspartame in cakes without added sugar. *Food Chemistry, 63*(1), 33–37.

Yan, B., Davachi, S. M., Ravanfar, R., Dadmohammadi, Y., Deisenroth, T. W., Pho, T. V., et al. (2021). Improvement of vitamin C stability in vitamin gummies by encapsulation in casein gel. *Food Hydrocolloids, 113*. https://doi.org/10.1016/j.foodhyd.2020.106414

Ye, F., Yang, R., Hua, X., Shen, Q., Zhao, W., & Zhang, W. (2013). Modification of stevioside using transglucosylation activity of Bacillus amyloliquefaciens α-amylase to reduce its bitter aftertaste. *Lebensmittel-Wissenschaft und -Technologie- Food Science and Technology, 51*(2), 524–530.

Ye, F., Yang, R., Hua, X., Shen, Q., Zhao, W., & Zhang, W. (2014). Modification of steviol glycosides using α-amylase. *Lebensmittel-Wissenschaft und -Technologie- Food Science and Technology, 57*(1), 400–405.